

## Facing the Challenges of Borderline Oxidation State Assignments Using State-of-the-Art Computational Methods

Martí Gimferrer, Jeroen Van der Mynsbrugge, Alexis T. Bell, Pedro Salvador, and Martin Head-Gordon\*

Cite This: *Inorg. Chem.* 2020, 59, 15410–15420

Read Online

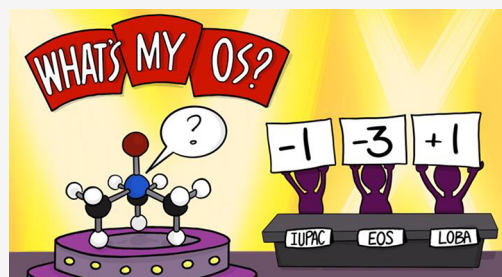
ACCESS |

Metrics &amp; More

Article Recommendations

Supporting Information

**ABSTRACT:** The oxidation state (OS) of metals and ligands in inorganic complexes may be defined by carefully curated rules, such as from IUPAC, or by computational procedures such as the effective oxidation state (EOS) or localized orbital bonding analysis (LOBA). Such definitions typically agree for systems with simple ionic bonding and innocent ligands but may disagree as the boundary between ionic and covalent bonds is approached, or as the role of ligand noninnocence becomes nontrivial, or high oxidation states of metals are supported by heavy dative bonding, and so on. This work systematically compares IUPAC, EOS, and LOBA across a series of complexes where OS assignment is challenging. These systems include high-valent transition metal oxides, transition metal complexes with noninnocent ligands such as dithiolate and nitrosyl, metal sulfur dioxide adducts, and two transition metal carbene complexes. The differences in OS assignment by the three methods are carefully discussed, demonstrating the synergy between EOS and LOBA. In addition, a clarity index for LOBA OS assignments is introduced that provides an indication of whether or not its predictions are close to the ionic–covalent boundary.



## INTRODUCTION

One of the most fundamental chemical concepts is the oxidation state (OS), which is widely used for the rationalization, characterization, categorization, and prediction of reactivity of inorganic compounds. However, despite being universally taught and used, a well-established definition for this concept is still lacking. Informally, the oxidation state of an element (typically a metal) in a compound is the net charge that results from an ionic division of electrons and electron pairs between the selected element and the remainder of the molecule.

For years, the OS assignment was performed following a set of agreed upon rules, but without having an explicit definition of the concept. Recently, a new generic definition of OS has been entered into IUPAC's Gold Book, which reads as the *atom's charge after ionic approximation of its heteronuclear bonds*.<sup>1,2</sup> For homonuclear bonds, its electrons must always be divided equally, independently of the chemical environment. For assigning OS in molecular systems, the IUPAC algorithm starts by establishing the appropriate Lewis structure of the molecule. Then, each electron pair between bonded atoms is assigned to the more electronegative one, representing the simplest application of the ionic approximation. The atomic electronegativities are evaluated according to Allen's scale.<sup>3</sup>

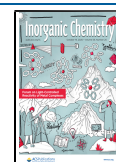
The new OS definition represents a large improvement compared with the previous set of rules. However, some limitations have already been exposed.<sup>4,5</sup> One example is the case of the transition metal (TM) carbenes.<sup>6</sup> In these systems, the carbene unit exhibits a double bond with the metal center. Because the carbene carbon atom is more electronegative than

the metal, the four electrons of the C=M double bond should be assigned to the carbon atom, leading to a formal C (−2). Thus, following IUPAC's rule, all carbene systems are assigned as Schrock-type. However, other carbene types exist, for instance the Fischer-type, which presents a neutral carbene moiety. One way to account for this OS assignment is to consider the  $\sigma$ -type bond polarized toward the C and the  $\pi$ -type to the metal center, giving two electrons to each moiety. This view cannot be reconciled with IUPAC's winner-takes-it-all rule, so classifying a carbene as Fischer-type requires approaches beyond IUPAC's ionic approximation. Another example is the nitrosyl-containing compounds.<sup>7</sup> In this case the nitrosyl–metal bonding relies on three interactions: one formal  $M \leftarrow NO^+$  sigma donor bond of virtually pure ligand character that the ionic approximation assigns to the NO and two  $M-\pi^*(NO)$  bonds whose character may vary between the limiting  $M \leftarrow NO^-$  and  $M \rightarrow NO^+$  scenarios. These two interactions are highly covalent, resulting in ambiguous OS assignments.<sup>8</sup> Furthermore, the  $NO^0$  picture is not supported by the ionic approximation.

Arguably, the most important limitation of IUPAC's algorithm is the inability of the atomic electronegativity scale

Received: August 12, 2020

Published: October 8, 2020



to account for differences in the local chemical environment. A plausible solution is to define atom types, as commonly used in force fields for molecular dynamics, with associated electronegativity values. However, the complexity of the algorithm will increase rapidly, lowering its practical utility. From our perspective, the OS must be connected to the electron distribution around the atoms. Today, modern electronic structure methods can accurately describe the electron density, which makes computational chemistry a natural candidate to aid in elucidating oxidation states.

A common misconception is that atomic charges from population analysis are a noninteger form of the OS. While one can still find atomic charges being used in the literature for OS assignment,<sup>9–11</sup> more appropriate computational methods for OS assignment treat electrons by pairs (in the case of pure singlet states) or individually (for open-shell systems). Then, each scheme applies one or another strategy to assign the electrons to atoms/fragments.

Some approaches are based on the use of localized occupied orbitals,<sup>12–15</sup> although the localization procedure is of course not unique. For single-determinant wave functions, one can perform unitary transformations on the occupied canonical orbitals, obtaining different localized orbitals without changing the wave function or energy. If a molecule is well-described by a single Lewis structure, we would expect the localized orbitals to fall into three categories: fully localized and atomic core orbitals, bonding orbitals that are shared between a pair of atoms (perhaps not equally, depending on their electronegativity difference), and nonbonding orbitals which are again completely atom-localized (e.g., lone pairs). However, more complex bonding patterns, like delocalized electrons shared between more than two atoms, can be encountered.

Within this family of methods, Thom et al. proposed the localized orbitals bonding analysis (LOBA), based on combining orbital localization with atomic population analysis to extract the OS from transition metal complexes.<sup>12</sup> Concretely, first the electronic structure of the complex is obtained at a single-determinant level. Then, the occupied molecular orbitals (MOs) from the system are localized following the desired localization procedure, e.g., Pipek–Mezey<sup>16</sup> or Edminston–Ruedenberg.<sup>17</sup> Afterward, atomic population analysis, e.g., Mulliken,<sup>18</sup> Löwdin,<sup>19</sup> or Hirshfeld-type,<sup>20</sup> for each localized orbital is performed. Finally, the integer number of electrons from the orbital (two in the case of closed-shell and one for open-shell wave functions) is assigned to the selected atom if its population surpasses a given threshold. To date, the method aims to evaluate the OS of metals within transition metal complexes, and the threshold is set at 60%. If an orbital exhibits a population lower than 60%, its electrons are strictly assigned to the rest of the molecular system. Thus, LOBA directly provides the OS of the heavy (or selected) atoms within the complex. To assign the OS of the fragments, it is necessary to evaluate the shape of the localized orbitals and their atomic populations.

Similar strategies have been developed by Sit et al.<sup>13</sup> and later applied by Vidossich et al.<sup>14</sup> Sit et al. used maximally localized Wannier functions<sup>21</sup> as localized orbitals and obtained the corresponding centroids. Then, they used the position of the centroids to assign the electron pairs to the closest atom (closest-atom strategy). Vidossich et al. applied the same strategy, relying instead on the Pipek–Mezey (PM) localized orbitals. Recently, an extension to this procedure was explored by some of us,<sup>15</sup> whereby the 3D-space was

partitioned into atomic domains, and the electron pair from each localized orbital is assigned to the atomic basin where the orbital centroid is situated (basin-allegiance strategy). Even though the latter scheme performed better, it still failed on the TM carbenes.

Alternatively, Ramos-Cordoba et al. introduced the effective oxidation state (EOS) analysis, which is formally applicable to any molecular system and wave function.<sup>22</sup> The scheme relies on Mayer's effective fragment orbitals (EFOs) obtained for each fragment/atom defined and their occupation number ( $\lambda$ ).<sup>23,24</sup> Once the spin-resolved EFOs are obtained, they are sorted by decreasing occupation number, and individual electrons are assigned to them until reaching the total system number of electrons. This procedure leads to an effective configuration of the ligands/atom within the molecule and, as a consequence, its OS. Furthermore, the difference between occupation numbers from the last occupied (LO) and first unoccupied (FU) EFOs is used to evaluate the reliability of the assignment. The larger this difference, the better the current electron distribution can be pictured as a discrete ionic model. This reliability index,  $R(\%) = \min(R_\omega, R_\beta)$ , is defined for each spin case  $\sigma$  as

$$R_\sigma(\%) = 100 \cdot \min(1, \max(0, \lambda_{\text{LO}}^\sigma - \lambda_{\text{FU}}^\sigma + 1/2)) \quad (1)$$

By definition, if the difference between occupation numbers of the frontier EFOs is larger than half an electron, the OS assignment is considered as undisputable ( $R(\%) = 100$ ). The worst-case scenario is in case that two or more frontier EFOs from different fragments present the same occupancy. In this case, two different equally plausible OS distributions are present with  $R(\%) = 50$ . Reliability index values lower than 50 are only possible if the electrons have not been assigned following the *aufbau* principle. Such assignments can be used to quantify to which extent the molecular system conforms to a given set of predefined OSs.

Both EOS and LOBA methodologies have been successfully applied by several authors to a broad range of chemical systems, proving their usefulness.<sup>25–27</sup> However, to date, there has been no comparison between the two schemes. Such a comparison with reference assignments (IUPAC, experimental characterization and/or previous assignments using alternative strategies) allows us not only to evaluate the synergy between both but also to critically evaluate the reference OS.

In this work, we first reformulate the use of population analysis within the LOBA scheme by including the definition of an index which quantifies the clarity in our OS assignments. Herein, we support the idea of assigning the electrons of localized orbitals ionically when the atomic populations are truly unbalanced, as observed by clarity index values larger than e.g. 70. The remaining electrons to assign require consideration of the localized orbital shape, based on chemical intuition. Thus, we remove the dependencies on population analysis method used (Mulliken, Löwdin, or Hirshfeld, among others) and rigidity of using a single population value as threshold, increasing the robustness of the method. Second, we computationally assign using both schemes the OS of 20 molecular systems of varying chemical nature and complexity, including high-valence transition metal oxides, transition metal complexes with noninnocent ligands, metal sulfur dioxide adducts, and transition metal carbene complexes. The majority of these systems have been already characterized by means of EOS by using the X-ray geometries when available.<sup>4,6</sup> Here, we

re-evaluate the EOS results using the wb97X-V/def2-TZVP optimized geometries for robustness of the production results.

## RESULTS AND DISCUSSION

**Reliability Index for the LOBA Method.** As mentioned above, LOBA requires the use of a population analysis threshold to assign the electrons from a localized orbital to either the metal center or the rest of the molecular system. Prior studies have shown that setting the population threshold to 60% yields satisfactory performance for the systems tested.<sup>12,26</sup> However, the chosen systems typically had well-defined OS. By contrast, when facing compounds with nontrivial bonding situations, the number of electrons from localized orbitals with atomic populations close to the borderline 50–70% region increases. In this regime, there may be scope for different interpretations from the same computational result, since a small geometric change can interconvert two different OS by crossing the LOBA threshold.

To quantify the extent to which LOBA OS assignments are clear-cut, we introduce a new clarity index,  $CI_a$ . First, we define the following quantity,  $x$ , from the population analysis performed for every localized orbital

$$x = \frac{\text{abs}(\lambda_M - \lambda_X)}{\lambda_M + \lambda_X} \quad (2)$$

where  $\lambda_M$  corresponds to the atomic population of the selected atom (e.g., the metal center, for the case of transition metal complexes) and  $\lambda_X$  is the population of the rest of the molecular system. With this definition, the parameter  $x$  is bounded within the  $[0, 1]$  range, independently of the wave function being closed or open shell. As limits, the  $x = 1$  case is when the orbital population is completely on either the selected atom M or on the rest of the molecular system X, while  $x = 0$  corresponds to the  $\lambda_M = \lambda_X$  scenario.

Next, we define a parameter  $P$ , which corresponds to a threshold for ionicity, to separate the assignment of the electrons of a given localized orbital into two ranges depending on the  $x$  value obtained (Figure 1): covalent ( $0 < x < P$ ) and ionic ( $P < x < 1$ ). In the ionic range, the electrons in the localized orbital are entirely assigned to M if  $(\lambda_M - \lambda_X) > 0$  or to the rest of the molecular system X if  $(\lambda_M - \lambda_X) < 0$ . In the covalent (or shared-pair) range, the electrons in the orbital are split equally between the two moieties.

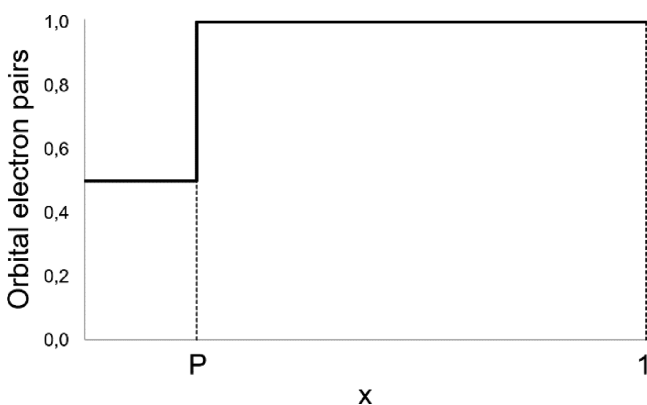


**Figure 1.** Plot of the assignment of the electrons in a localized orbital for  $x \in [0, 1]$ , where  $x$  is defined by eq 1. The covalent regime is  $0 < x < P$  while the ionic regime is  $P < x < 1$ .

Finally, to quantify the extent to which the assignment is clear, we introduce a second parameter,  $W$ , which corresponds to the width for switching the electronic assignment from ionic to covalent. Using  $x$  and the parameters  $P$  and  $W$ , we define the new clarity index,  $CI_a$ , where  $a = i$  for ionic and  $a = c$  for covalent assignments, in three ranges:  $CI_c = 100$  for  $x \in [0, P - W]$ ,  $CI_i = 100$  for  $x \in [P + W, 1]$ , and  $CI_a = CI_a(x)$  within the  $x \in [P - W, P + W]$  interval. With all conditions set, a plausible form for  $CI_a(x)$  is

$$CI_a(x) = 100 \cos^2\left(\pi\left(\frac{P + W - x}{2W}\right)\right) \quad (3)$$

which is a smooth, continuous function with a symmetrical shape (Figure 2) and a rather simple mathematical expression.

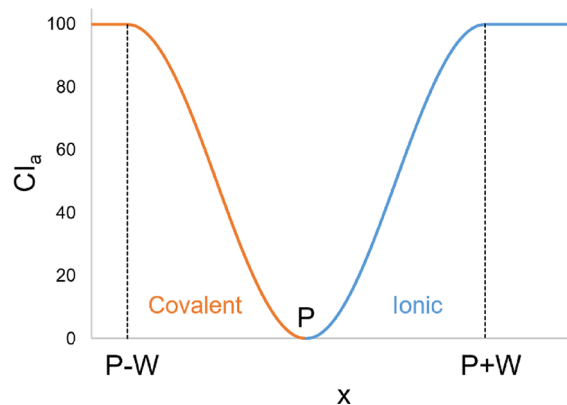


**Figure 2.**  $CI_a(x)$  index representation.

Herein, we use  $P = 0.2$  and  $W = 0.1$ . This  $P$  choice corresponds to the  $x$  value for the original population threshold (60%), while the selected  $W$  value is based on the population threshold calibration calculations performed in ref 12; it matches the region which minimizes the error on the OS assignment.

By definition, a  $CI_a$  value is obtained for each localized orbital, reflecting the clarity in the assignment of the electron(s) from that orbital. Evidently, the least clearly assigned electrons in the molecular system will determine how conclusive the final OS assignment will be. For this reason, we ultimately select the lowest  $CI_a$  value as the most conservative indicator of our overall OS assignment clarity.

**Illustrative Examples.** To evaluate the strengths and weaknesses of the EOS and LOBA methods, we have considered a series of compounds that present challenges when it comes to making OS assignments. The selected compounds include high-valent transition metal oxides, transition metal complexes with noninnocent ligands (thiolate, nitrosyl, and (presumably) trifluoromethyl), transition metal sulfur dioxide adducts, and transition metal carbene complexes. We discuss in detail the OS assignments obtained from both the EOS and LOBA methods and compare them with reference values (typically given by IUPAC's ionic approximation). We also evaluate the performance of the newly introduced LOBA clarity index  $CI_a$ .<sup>1,2</sup>

**Trimethylamine N-Oxide.** Before discussing various transition metal complexes, let us first discuss the relatively simple molecule trimethylamine N-oxide,  $(\text{CH}_3)_3\text{NO}$ . The dominant Lewis structure for this system presents a single bond between formal N (+) and O (−), as N fulfills the octet rule. Applying

IUPAC's ionic approximation, all electrons (by pairs, as  $(\text{CH}_3)_3\text{NO}$  is a closed-shell system) from the  $\sigma$  N–C bonds are assigned to N, while the ones from the N–O bond are assigned to the oxygen. Such an electron assignment leads to formal oxidation states of (–1) for N, (–2) for O, and (+1) for the three  $\text{CH}_3$  moieties.

From the EOS perspective, we obtained the OS assignment of N (–3), O (0), and each  $\text{CH}_3$  (+1) with  $R$  (%) = 55.7. The same result was previously reported,<sup>4</sup> with small differences in  $R$  (%) because of the different level of theory and geometry used here versus in ref 4. We quantified the weight of IUPAC's N (–1) and O (–2) assignment by not following the *aufbau* principle on the electron assignment, resulting in  $R$  (%) = 44.3.

When analyzing the shape of the PM localized orbitals, no localized orbital corresponding to a  $\pi$ -type N–O bond is found, but two lone pairs localized on O are present. This points to the aforementioned Lewis structure. In this direction, some of us assigned its OS using the position of the centroids of the localized orbitals. They obtained the EOS assignment from both the closest-atom and basin-allegiance strategies.<sup>15</sup> This result is in contradiction with the IUPAC assignment, and further analysis is warranted.

We performed LOBA calculations and depict the shape of selected PM localized orbitals, together with their Löwdin population analysis and  $\text{Cl}_a$  values in Figure 3. Each localized

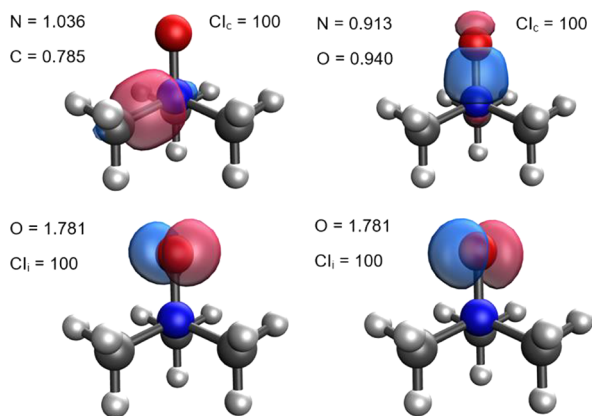


**Figure 3.** Selected valence PM localized orbitals for the  $(\text{CH}_3)_3\text{NO}$  molecular system, together with Löwdin population and  $\text{Cl}_a$  values. The isocontour value is selected for clarity as 0.3 au.

orbital accounts for an electron pair as the system is closed-shell. Visual inspection shows two lone pairs localized on O and localized  $\sigma(\text{NO})$  and  $\sigma(\text{CN})$  bond orbitals. Evaluating the orbital shape, both localized  $\sigma$  orbitals are characterized as shared-pair, resulting in assigning one electron to each atom involved (per orbital). Such an assignment leads to N (+1), O (–1), and each  $\text{CH}_3$  (0). When evaluating the reliability of our assignments, we obtain the covalent assignment for both  $\sigma(\text{N–C})$  and  $\sigma(\text{N–O})$  orbitals with  $\text{Cl}_c = 100$ . This assignment is different from both the IUPAC and EOS results. The LOBA  $\sigma(\text{N–O})$  assignment can only be supported by EOS in the case of occupation degeneracy of the frontier EFOs. In this situation, one electron is assigned into each EFO, mimicking the covalent (shared-pair) assignment. Thus, the closer the frontier EFOs occupancies, the more shared-pair “character”. However, EOS clearly assigned each  $\text{CH}_3$  moiety as (+1).

**High-Valent Transition Metal Oxides.** Our first group of transition metal complexes consists of a series of high-valent

transition metal oxides, including  $\text{TiO}_2$ ,  $\text{FeO}_4^{2-}$ ,  $\text{ReO}_4^-$ ,  $\text{OsO}_4$ ,  $\text{IrO}_4^+$ , and  $\text{PtO}_4^{2+}$ .<sup>28,29</sup> According to the IUPAC's ionic approximation, such species present a rich variety of metal oxidation states ranging from (+4) to (+10). Prior studies showed very good performance for this systems by EOS, as compared to OS assignments following IUPAC's rules, resulting in formal OS values up to (+9) for Ir in  $\text{IrO}_4^+$ .<sup>4</sup> In the case of  $\text{PtO}_4^{2+}$ , the Pt atom presented several d-type EFOs with occupations too large to be considered empty, compared to those of the O atoms, and the EOS scheme assigned Pt (+2) with  $R$  (%) = 50.8. By contrast, at the current level of theory, EOS achieves the (+6) OS assignment for Pt, again with a very small  $R$  (%) = 50.3 value. This method dependency makes the system a matter of interest, particularly as we have previously demonstrated the robustness of the EOS method for an extensive combination of functionals and basis sets.<sup>6</sup> Considering the  $\omega\text{B97X-V}/\text{def2-TZVP}$  description at the geometry reported in ref 4 leads to a Pt (+2) assignment, with  $R$  (%) = 52.8. Thus, disagreement on the assignment is mostly caused by geometrical differences. Nevertheless, it appears that the use of more sophisticated long-range corrected DFT functionals such as  $\omega\text{B97X-V}$ , which include a density-dependent dispersion correction, may increase the ionic character of each bond by lowering the delocalization error. The more ionic the bonds, the more oxidized is the character of the metal center.

In Figure 4 we depict the valence PM orbitals corresponding to one  $\sigma(\text{M–O})$  bond for each complex. By symmetry, the

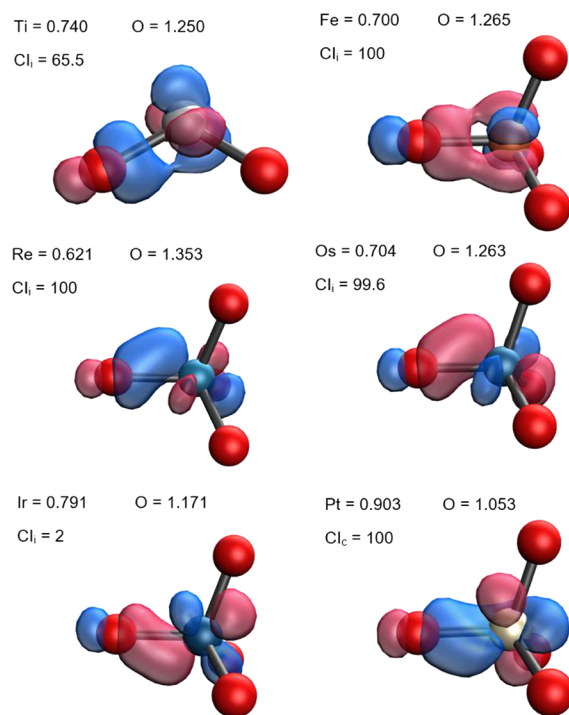


**Figure 4.** Selected valence PM localized orbitals for  $\text{TiO}_2$ ,  $\text{FeO}_4^{2-}$ ,  $\text{ReO}_4^-$ ,  $\text{OsO}_4$ ,  $\text{IrO}_4^+$ , and  $\text{PtO}_4^{2+}$  molecular systems, together with Löwdin population and  $\text{Cl}_a$  values. The isocontour value is 0.3 au.

orbital picture and population analysis are equal for all  $\sigma(\text{M–O})$  bonds. Differences between atomic populations become less clear when going to higher valent compounds, not only from LOBA but also from the  $R$  (%) values close to 50 from EOS. The electron pair from the  $\sigma(\text{M–O})$  bonds is assigned to

the O atom for all systems, as the atomic populations differences are large enough, except for  $\text{PtO}_4^{2+}$ . In  $\text{PtO}_4^{2+}$ , population analysis and localized orbital shape support a covalent assignment for the Pt–O pairs. Thus, as by symmetry there are four electron pairs in this situation, assigning one electron to each moiety leads to a formal OS for Pt (+6) and each O (–1). Covalent assignment is confirmed, with  $\text{CI}_c = 100$ . Interestingly, the OS assignment for the Ir-based oxide is at the frontier between covalent and ionic assignment, being ionic with a pyrrhic  $\text{CI}_i = 2$ . The Ir and Pt systems show the way in which extremely high formal IUPAC oxidation states play out via the orbital shape.

**Transition Metal Complexes with Noninnocent Ligands.** Next, we consider OS assignments for different families of transition metal complexes with noninnocent ligands such as thiolate, nitrosyl, and trifluoromethyl. Our first set of noninnocent ligand complexes consists of the redox series of nickel dithiolates  $[\text{Ni}(\text{S}_2\text{C}_2\text{Me}_2)]^{n-}$ , with  $n = 0, 1$ , and 2.<sup>30</sup> From experiments and DFT calculations, Lim et al. characterize the dianionic species as a Ni (+2) metal center with two closed-shell thiolate (–2) ligands. Furthermore, the one-electron oxidations on this species are ligand based, such that the Ni OS remains constant throughout the redox process.<sup>31</sup> Particularly, for  $n = 1$ , the reference OS for the thiolate ligands can be either –1/–2 (asymmetric assignment) or –1.5/–1.5 (mixed valence). Finally, the neutral species presents two formally (–1) thiolate ligands.

EOS analysis matches the reference OS with  $R$  (%) values of 55.7, 65.7, and 82.4 for the 0, 1, and 2 species, respectively. The most interesting case is the lower  $R$  value neutral species. Here, as the system is closed-shell, the only manner by which the (–1) OS solution can be obtained is if the two last occupied EFOs are degenerate in occupancy and are located one on each ligand, thus splitting the electron pair between both fragments. Wave function stability analysis confirmed that the ground state solution is closed-shell. We obtained the described scenario, with two degenerate EFOs (occupancy 0.51), one from each ligand, and a Ni EFO (occupancy 0.45). An alternative, though unfaithful, assignment is a Ni (0) center with two neutral ligands, resulting in a  $R$  (%) value of 44.3.

LOBA also assigns the Ni center as (+2) with  $\text{CI}_i = 100$ , as the Ni atom presents four d-type localized orbitals, two fewer electrons than a formal Ni (0). With regard to the ligands, we obtain two formal (–1) dithiolates. Obtaining this solution from localized orbitals is more complicated than from EOS, as a single doubly occupied orbital must be delocalized between the two ligands. In particular, that orbital must present atomic populations that are split between four atoms (at least). We depict the aforementioned orbital in Figure 5, observing a shared-pair character and thus leading to the (–1) OS for each

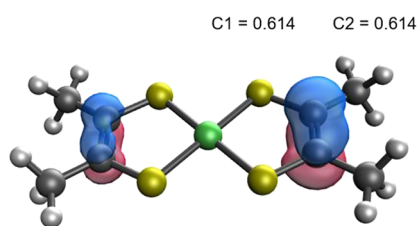


**Figure 5.** PM localized orbital between both noninnocent ligands of the  $[\text{Ni}(\text{S}_2\text{C}_2\text{Me}_2)]^0$  system, together with the Löwdin population. The isocontour value is 0.15 au.

ligand. However, the localized orbital is not truly symmetric between fragments, giving some weight to the asymmetric (0)/(–2) assignment. Using the sum of carbon populations in the right fragment against the total, the asymmetric assignment is obtained with  $\text{CI}_i = 18.1$ . As the complementary localized orbital can be obtained by an alternative combination of MOs, the asymmetric assignment in this case is caused by the difficulty to localize the orbital, resulting in a broken symmetry representation of a symmetric bonding situation.

For  $n = 2$ , LOBA shows a similar orbital pattern and the same Ni OS assignment. Instead of one localized orbital split between both ligands (as in Figure 5), we find a fully localized one for each ligand. Thus, we obtain two formal (–2) ligands. Finally, in the  $n = 1$  case the ground state multiplicity is a doublet. Consequently, alpha and beta localized orbitals are treated independently. It is worth mentioning that at the present level of theory the spin density is almost perfectly shared among the Ni and each of the ligands (0.34, 0.33, and 0.33, respectively). In the LOBA approach, the  $\sigma$  Ni–S bond electrons are assigned to S by both population analysis and orbital shape (Figure 6). The Ni center presents  $4\alpha$  and  $3\beta$  d

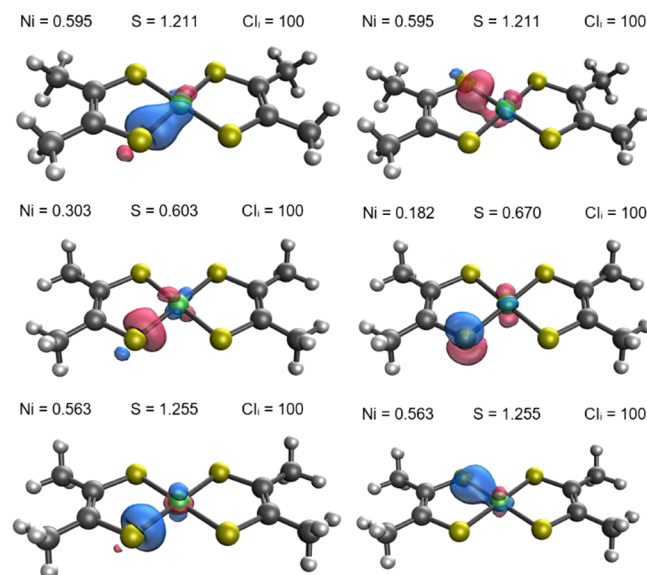


**Figure 6.** Selected PM localized orbitals for  $[\text{Ni}(\text{S}_2\text{C}_2\text{Me}_2)]^{n-}$  molecular systems,  $n = 0$  (top), 1 (middle; alpha, left, and beta, right), and 2 (bottom), together with Löwdin population and  $\text{CI}_i$  values. The isocontour value is 0.3 au.

localized orbitals, leading to a formal Ni (+3) species with  $\text{CI}_i = 100$ . Such an assignment opposes both the reference results and the EOS values, as LOBA instead hints at a metal-based oxidation instead of ligand-based. It is important to note that obtaining a nonsymmetric (or mixed-valence) OS assignment from a geometrically symmetric system is a challenge for any methodology. In the EOS case, there are two degenerate EFOs, one per thiolate ligand, and only one electron left to assign. Thus, the splitting of the last electron leads to the –1.5/–1.5 (mixed-valence) result. Alternatively, one may consider two equivalent resonance structures with OS of –2/–1 and –1/–2 for the ligands. For this set of systems, limitations of the LOBA scheme are observed, but these limitations derive from challenges in orbital localization and not from the OS assignment procedure or the  $\text{CI}_i$  index definition.

As a second set of transition metal complexes with noninnocent ligands, we considered the redox couple of nitroprusside anions  $[\text{Fe}(\text{CN})_5(\text{NO})]^{n-}$ ,<sup>32</sup> where  $n = 2, 3$ . NO is a simple noninnocent ligand that can present three different oxidation states,  $-1, 0$ , or  $+1$ , depending on its interaction with the metal center. For its OS assignment, IUPAC's statement is clear: *the MNO segment should be linear for  $\text{NO}^+$  but bent for  $\text{NO}^-$* .<sup>7</sup> For  $n = 2$ , the geometry of the complex indicates a linear FeNO segment. Thus, according to IUPAC's rule, the NO is formally  $(+1)$ . Then, from the ionic approximation each CN ligand is  $(-1)$ , leading to a formal Fe  $(+2)$  OS. Applying the same rules, the bent geometry of the FeNO linkage in the  $n = 3$  system is characteristic of NO  $(-1)$ . However, the last system is properly characterized as neutral NO, which leads to a formal Fe  $(+2)$ .<sup>32</sup>

EOS analysis reproduced the reference OS for both species with  $R (\%) = 81.0$  and  $74.0$ . From LOBA, for both  $n = 2$  and  $3$ , the  $\sigma(\text{Fe}-\text{C})$  localized orbitals are ionically assigned to the CN moiety with  $\text{CI}_i = 100$ , thus leading to the CN  $(-1)$  OS assignment. In the  $n = 2$  system, the two localized orbitals from the Fe–N interaction (Figure 7) are assigned to the iron

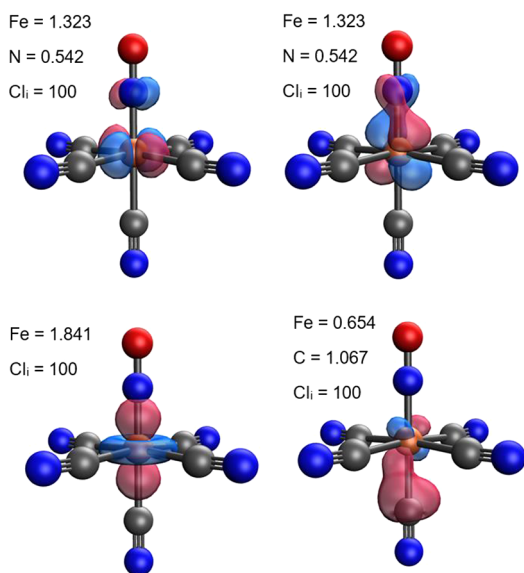


**Figure 7.** Selected valence PM localized orbitals for  $[\text{Fe}(\text{CN})_5(\text{NO})]^{2-}$  molecular system, together with its Löwdin population and  $\text{CI}_i$  values. The isocontour value is  $0.30 \text{ au}$ .

center with a clear  $\text{CI}_i = 100$ . This together with a Fe-centered d-type localized orbital leads to the formal Fe  $(+2)$  OS. As a consequence, the NO moiety is then characterized as  $(+1)$ .

For  $n = 3$ , with spin unrestricted localized orbitals depicted in Figure 8, the Fe exhibits  $2\alpha$  and  $3\beta$  d-type orbitals, which, together with the nontrivial assignment of the Fe–N interaction to the iron ( $\text{CI}_i = 28.7$  (alpha)), lead to the  $(+2)$  OS for Fe. As a consequence, the NO ligand is characterized as neutral. These results are in perfect agreement with both reference values and EOS analysis.

A final set of systems within this category are the copper trifluoromethyl complexes  $[\text{Cu}(\text{CF}_3)_4]^{n-}$ , with  $n = 1, 2$ , and  $3$ . For  $n = 1$ , Snyder characterized computationally the metal center as a formal Cu  $(+1)$ , leading to one  $\text{CF}_3$   $(+1)$ , one  $(-1)$ , and two formally  $(-0.5)$ .<sup>33</sup> Several authors argued against this assignment, pointing instead to a formally Cu  $(+3)$  species.<sup>34,35</sup> Recent experimental evidence seems to point

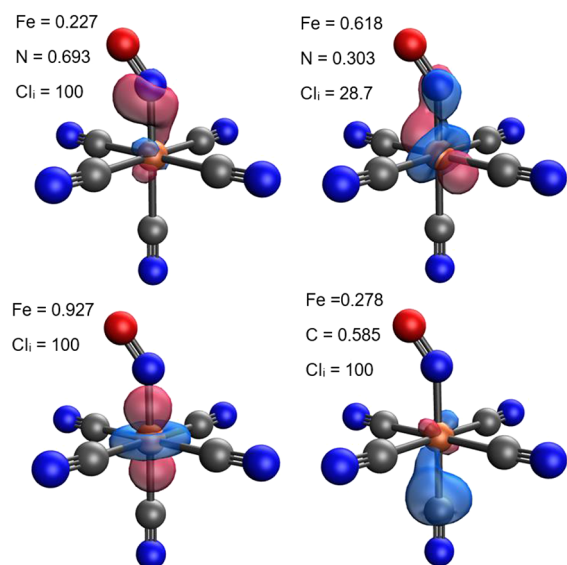


**Figure 8.** Selected valence PM localized orbitals for  $[\text{Fe}(\text{CN})_5(\text{NO})]^{3-}$  molecular systems (alpha spin), together with Löwdin population and  $\text{CI}_i$  values. The isocontour value is  $0.30 \text{ au}$ .

toward a Cu  $(+1)$  metal center,<sup>36,37</sup> casting doubts on the mere existence of any Cu  $(+3)$  species. At any rate, the OS assignment of this system has proved challenging because of the significant covalency of the Cu–C bonds. One can even find studies where authors opt for different interpretations/assignments within the same work.<sup>38</sup> According to the ionic approximation, each  $\text{CF}_3$  ligand should present the  $(-1)$  OS in all species, leading to Cu  $(+3)$  for the  $n = 1$  system, which is successively reduced to Cu  $(+1)$  for  $n = 3$ .

EOS analysis assigns the OS of Cu in the  $n = 1$  species  $(+3)$  with  $R (\%) = 51.7$ , which is at odds with a recent combined experimental–computational interpretation.<sup>36</sup> It is particularly striking to notice that the authors used virtually the same level of theory as in this work but arrived at different conclusions. On the other hand, the low  $R$  value obtained is indeed indicative of the high covalency of the Cu–C bond. An alternative assignment consists of assigning two electrons from the four pseudo-degenerate LO EFOs, each one located on a  $\text{CF}_3$  moiety, to Cu. This leads to a formal Cu  $(+1)$  and four  $\text{CF}_3$   $(-1/2)$  with  $R (\%) = 48.3$ , supporting in some sense Snyder's original proposal and highlighting the delicate balance in assigning the OSs. For the reduced species, metal-based reduction is observed, leading to unambiguous EOS assignments of Cu  $(+2)$  and Cu  $(+1)$  with  $R (\%) = 78.5$  and  $100$  for  $n = 2$  and  $3$ , respectively.

According to LOBA, with selected localized orbitals depicted in Figure 9, the  $n = 1$  system is clearly characterized as a Cu  $(+3)$  species with high clarity ( $\text{CI}_i = 100$ ). The electron pair from each  $\sigma(\text{Cu}-\text{C})$  bond is assigned to the  $\text{CF}_3$  moiety, each of which is formally  $(-1)$ . This, together with the four d-type localized orbitals sitting on the Cu atom, provides a clear Cu  $(+3)$  assignment. For  $n = 3$ , we obtained the same assignment for the  $\sigma(\text{Cu}-\text{C})$  localized orbitals, but now five d-type localized orbitals from Cu are occupied, leading to Cu  $(+1)$  with four  $\text{CF}_3$   $(-1)$  ligands. In the  $n = 2$  system, the  $\alpha$  and  $\beta$  electrons from  $\sigma(\text{Cu}-\text{C})$  localized orbitals are assigned to the  $\text{CF}_3$  moiety, leading once again to a formal  $\text{CF}_3$   $(-1)$ . Five  $\alpha$  and four  $\beta$  localized orbitals are localized on Cu, giving the formal  $(+2)$  OS with  $\text{CI}_i = 100$ .

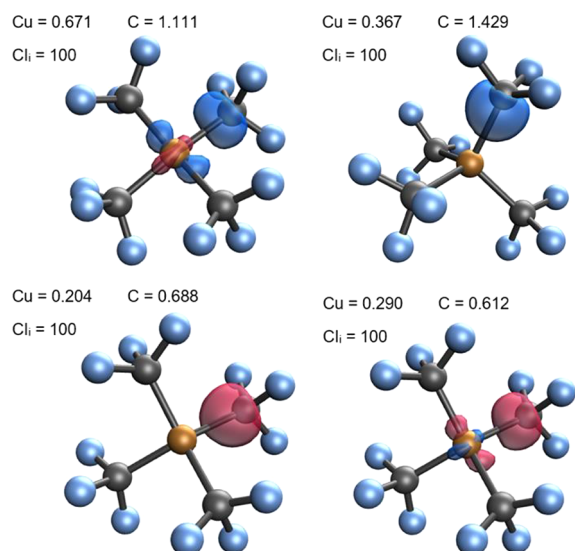


**Figure 9.** Selected valence PM localized orbitals for  $[\text{Cu}(\text{CF}_3)_4]^{n-}$  molecular systems,  $n = 1$  (top left), 3 (top right), and 2 (middle; alpha, left, and beta, right), together with Löwdin population and  $\text{CI}_a$  values. The isocontour value is 0.30 au.

In summary, both EOS and LOBA analysis characterize the  $[\text{Cu}(\text{CF}_3)_4]^-$  system as a Cu (+3)-based species and the subsequent reductions as metal-based. For  $n = 1$ , the EOS assignment is less clear than for the LOBA, which unambiguously assigned the Cu (+3) species. Clear assignments are obtained for the reduced species by using both schemes.

**Metal Sulfur Dioxide Adducts.** Another family of compounds we investigated are transition metal adducts with sulfur dioxide as a ligand.  $\text{SO}_2$  presents the ability to coordinate in three different manners (Z-, L-, and  $\pi$ -type). According to IUPAC, L-type ligands act as Lewis bases, donating the two electrons to the metal center to form a dative bond. Then, the ionic approximation assigns the electron pair to the S atom by electronegativity difference, leading to a neutral  $\text{SO}_2$ . For the Z-type, the ligand acts as a Lewis acid, and the metal atom sacrifices the electron pair for dative bond formation. Crude ionic approximation should lead to a formal  $\text{SO}_2$  (-2) ligand, which is at odds with the experimental observables. Thus, an exception to the ionic approximation is introduced to address such situations, which thereby leads to the expected neutral  $\text{SO}_2$ . Knowing when the exception should be invoked is perhaps challenging.

To explore the role of  $\text{SO}_2$  as a ligand, we selected the  $\text{Rh}(\text{SO}_2)\text{Cl}(\text{CO})(\text{PH}_3)_2$  (Z-type),  $\text{Rh}(\text{SO}_2)\text{Cl}(\text{PH}_3)_2$  (L-type), and  $\text{Ru}(\text{SO}_2)\text{Cl}(\text{NO})(\text{PH}_3)_2$  ( $\pi$ -type) systems to assign the OS of the metal and the  $\text{SO}_2$  ligands. Selected PM orbitals for these systems are depicted in Figures 10, 11, and 12, respectively.

For the Z-type ligand case of  $\text{Rh}(\text{SO}_2)\text{Cl}(\text{CO})(\text{PH}_3)_2$  (Figure 10), LOBA provides clear Rh (+1) and  $\text{SO}_2$  (0) assignments, with  $\text{CI}_i = 100$ . Furthermore, there is no localized orbital which, from population analysis, involves both Rh and S from  $\text{SO}_2$ . Rh presents four doubly occupied d-type localized orbitals, while  $\text{SO}_2$  obtains the 24 electrons required for being a neutral ligand. Clear-cut assignments are also obtained for all  $\text{PH}_3$ , CO, and Cl  $\sigma$ -like localized orbitals, which leads to these normally innocent ligands being formally (0), (0), and (-1), respectively, as expected.

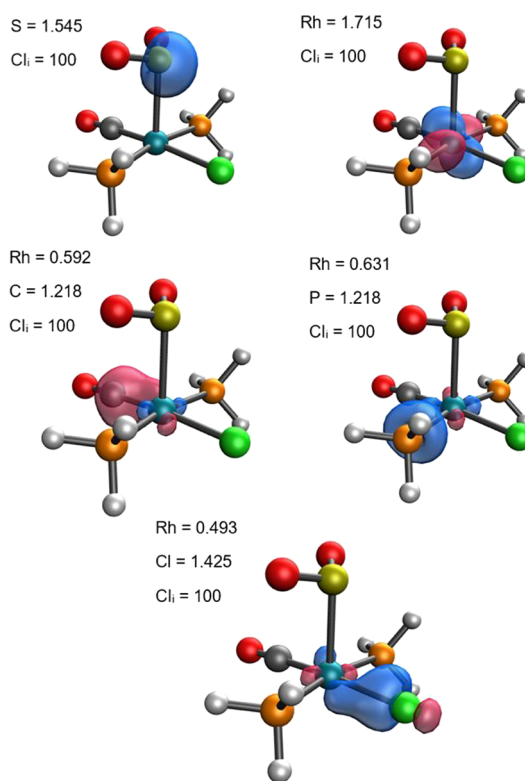


**Figure 10.** Selected valence PM localized orbitals for Z-type Rh-based compound,  $\text{Rh}(\text{SO}_2)\text{Cl}(\text{CO})(\text{PH}_3)_2$ , together with Löwdin population and  $\text{CI}_a$  values. The isocontour value is 0.30 au.

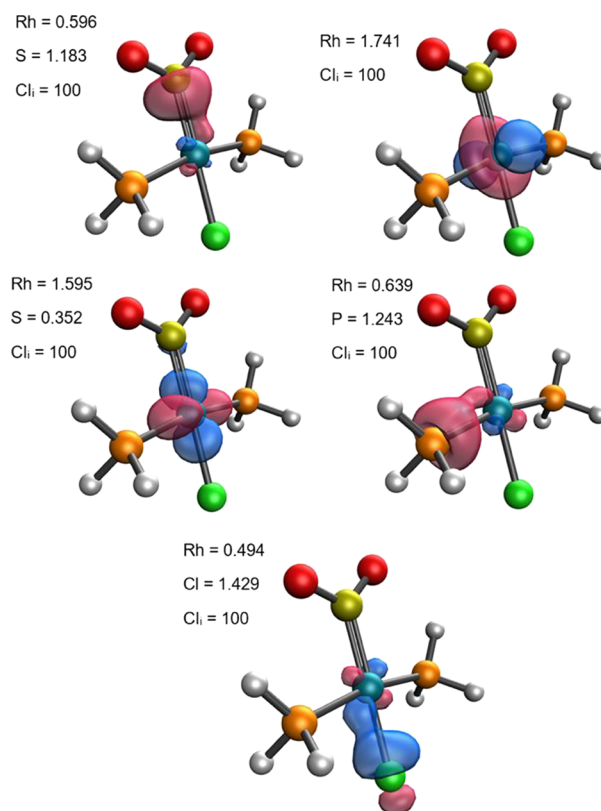


**Figure 11.** Selected valence PM localized orbitals for L-type Rh-based compound,  $\text{Rh}(\text{SO}_2)\text{Cl}(\text{PH}_3)_2$ , together with Löwdin population and  $\text{CI}_a$  value. The isocontour value is 0.30 au.

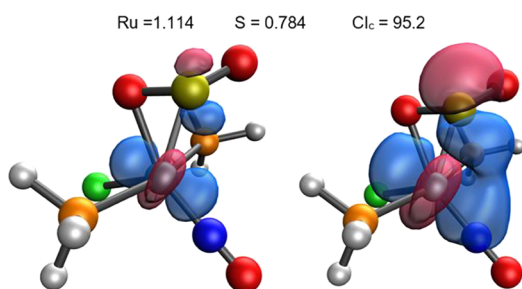


**Figure 12.** A selected valence PM localized orbital for the  $\pi$ -type Ru-based compound,  $\text{Ru}(\text{SO}_2)\text{Cl}(\text{NO})(\text{PH}_3)_2$ , together with Löwdin population and  $\text{Cl}_a$  value. Two isocontour values are used: 0.30 au (left) and 0.10 au (right).

For the L-type ligand case of  $\text{Rh}(\text{SO}_2)\text{Cl}(\text{PH}_3)_2$  (Figure 11), Rh presents three d-type localized orbitals and one resulting from the combination of a  $\sigma$ -type orbital from S and a d-type from Rh, leading to the formal (+1) OS with  $\text{Cl}_i = 100$ . The  $\text{SO}_2$  ligand is characterized as neutral, which is in nice agreement with the reference values. The  $\text{PH}_3$  and Cl ligands present the same conventional bonding situation as for the Z-type ligand.

Finally, a more complicated bonding situation is observed for the  $\pi$ -type case of  $\text{Ru}(\text{SO}_2)\text{Cl}(\text{NO})(\text{PH}_3)_2$ . Starting from the  $\text{SO}_2$  ligand, a nonbonding orbital between the Ru and S atoms is obtained (Figure 12), which is characterized as a shared pair with  $\text{Cl}_c = 95.2$ . Decreasing the isocontour value for this orbital, a weak  $\sigma$ -type interaction between the S of  $\text{SO}_2$  and the N of NO ligand is unveiled. Even though the localized orbital is shared between three atoms, it is mainly localized between the Ru and S, so that the NO is not involved in this particular electron assignment process.

The localized orbital from the Ru–O interaction (Figure 13) is ionically assigned to the O of  $\text{SO}_2$  with  $\text{Cl}_i = 100$ , meaning that  $\text{SO}_2$  is assigned as (–1). With regard to the NO ligand, the  $\pi(\text{Ru}–\text{N})$  localized orbital is characterized as a shared pair with  $\text{Cl}_c = 100$ , leading to a neutral NO moiety. Because the Cl

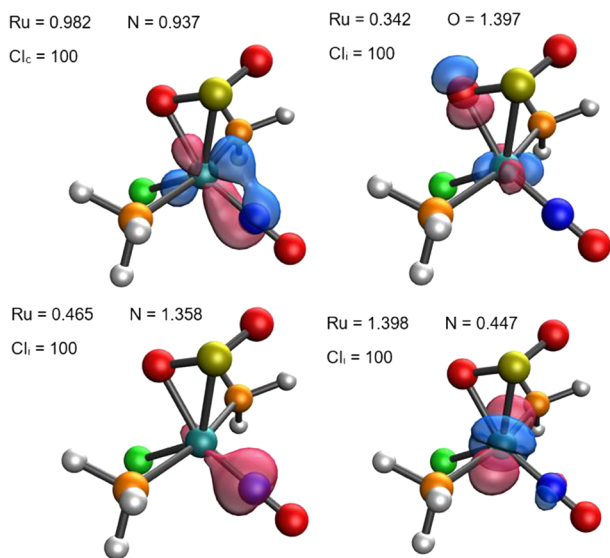


**Figure 13.** Selected valence PM localized orbitals for  $\pi$ -type Ru-based compound,  $\text{Ru}(\text{SO}_2)\text{Cl}(\text{NO})(\text{PH}_3)_2$ , together with Löwdin population and  $\text{Cl}_a$  values. The isocontour value is 0.30 au.

and  $\text{PH}_3$  ligands present their typical (–1) and (0) OS, respectively, the Ru center OS is (+2).

EOS analysis matched the reference OS for the  $\text{SO}_2$  moiety with  $R$  (%) = 85.2, 84.0, and 50.3 for the L-, Z-, and  $\pi$ -type, respectively. EOS is in agreement also with the LOBA assignments for the L- and Z-type compounds. In the  $\pi$ -type case, EOS also indicates a covalent assignment for the  $\sigma(\text{Ru}–\text{N})$  localized orbital, as the frontier EFOs between both fragments are almost degenerate in occupation number, leading to a formal NO (0) ligand. Contrary to LOBA, a clear  $\text{SO}_2$  (0) assignment, and consequently Ru (+1), has been obtained for the  $\pi$ -type species by EOS.

**Transition Metal Carbene Complexes.** The last two evaluated compounds are within the transition metal carbene family. In particular, we examine the Schrock-type compound,  $\text{Mo}(=\text{CH}_2)(\text{NC}_8\text{H}_{10})(\text{OtBu})_2$ , and the Fischer-type complex,  $\text{W}(=\text{CF}_2)(\text{CO})_5$ . As mentioned above, IUPAC's ionic approximation fails on elucidating the carbene moiety OS in the Fischer-type carbenes, assigning a formal (–2) OS instead of the accepted value of (0).

EOS analysis properly characterized the carbene moiety as (–2) for the Schrock-type compound with  $R$  (%) = 63.0 and as neutral for the Fischer-type species with  $R$  (%) = 96.6.

We depict the selected PM orbitals from the Fischer-type carbene,  $\text{W}(=\text{CF}_2)(\text{CO})_5$ , in Figure 14. There are two

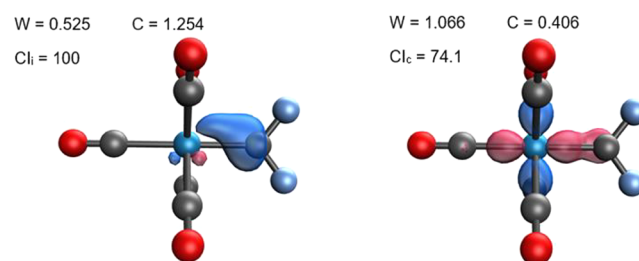


**Figure 14.** Selected valence PM localized orbital for  $\text{W}(=\text{CF}_2)(\text{CO})_5$ , together with Löwdin population and  $\text{Cl}_a$  values. The isocontour value is 0.30 au.

localized orbitals which describe the  $\text{W}=\text{C}$  bond. From LOBA, an ionic assignment with  $\text{Cl}_i = 100$  is obtained for the first, while the second has a covalent assignment with  $\text{Cl}_c = 74.1$ . These assignments lead to the carbene moiety having (–1) formal OS, instead of the expected (0).

For the Schrock-type complex,  $\text{Mo}(=\text{CH}_2)(\text{NC}_8\text{H}_{10})(\text{OtBu})_2$ , we depict the two localized orbitals that describe the  $\text{Mo}=\text{C}$  bond in Figure 15. Both orbitals are associated with a covalent assignment, with  $\text{Cl}_c = 33.1$  and 91.4. This

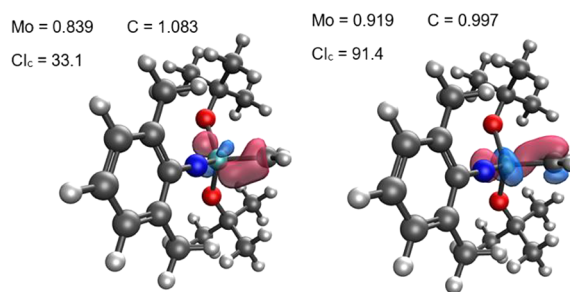


**Figure 15.** Selected valence PM localized orbital for  $\text{Mo}(=\text{CH}_2)(\text{NC}_8\text{H}_{10})(\text{OtBu})_2$ , together with its Löwdin population and  $\text{Cl}_a$  values. The isocontour value is 0.30 au.

results in a carbene unit with a formal OS of (0), which was the expected for a Fischer-type carbene. Here, the assignment of the four electrons from the Mo=C bond to the carbene moiety was expected.

EOS showed better performance for the carbene systems than LOBA. For the latter, these systems showed its primary challenge: the nonuniqueness of the localization procedure and the difficulty to obtain cleanly localized orbitals. Thus, more robust procedures need to be tested/developed before discarding the LOBA utility for this particular type of compound.

## CONCLUSIONS

In this work, we have examined the application of effective oxidation state (EOS) analysis and localized orbital bonding analysis (LOBA) to a series of compounds that present challenges in oxidation state (OS) assignment. Table 1

**Table 1. OS Assignments of the Atom/Ligand Indicated in Bold by EOS and LOBA<sup>a</sup>**

molecule	EOS	LOBA	IUPAC/ other
(CH <sub>3</sub> ) <sub>3</sub> NO <sup>b</sup>	-3 (55.7)	+1 (100)	-1
TiO <sub>2</sub>	+4 (92.6)	+4 (65.5)	+4
FeO <sub>4</sub> <sup>2-</sup>	+6 (68.9)	+6 (100)	+6
ReO <sub>4</sub> <sup>-</sup>	+7 (90.8)	+7 (100)	+7
OsO <sub>4</sub>	+8 (76.1)	+8 (99.6)	+8
IrO <sub>4</sub> <sup>+</sup>	+9 (60.2)	+9 (2)	+9
PtO <sub>4</sub> <sup>2+</sup>	+6 (50.3)	+6 (100)	+10
[Ni(S <sub>2</sub> C <sub>2</sub> Me <sub>2</sub> ) <sub>2</sub> ] <sup>0</sup>	+2 (55.7)	+2 (100)	+2
[Ni(S <sub>2</sub> C <sub>2</sub> Me <sub>2</sub> ) <sub>2</sub> ] <sup>1-</sup>	+2 (65.7)	+3 (100)	+2
[Ni(S <sub>2</sub> C <sub>2</sub> Me <sub>2</sub> ) <sub>2</sub> ] <sup>2-</sup>	+2 (82.4)	+2 (100)	+2
[Fe(CN) <sub>5</sub> (NO)] <sup>2-</sup>	+1 (80.9)	+1 (100)	+1
[Fe(CN) <sub>5</sub> (NO)] <sup>3-</sup>	0 (74.0)	0 (28.7)	0
[Cu(CF <sub>3</sub> ) <sub>4</sub> ] <sup>1-</sup>	+3 (51.7)	+3 (100)	+1/+3
[Cu(CF <sub>3</sub> ) <sub>4</sub> ] <sup>2-</sup>	+2 (78.5)	+2 (100)	+2
[Cu(CF <sub>3</sub> ) <sub>4</sub> ] <sup>3-</sup>	+1 (100)	+1 (100)	+1
Rh(SO <sub>2</sub> )Cl(CO)(PH <sub>3</sub> ) <sub>2</sub> (Z-type)	0 (84.0)	0 (100)	0
Rh(SO <sub>2</sub> )Cl(PH <sub>3</sub> ) <sub>2</sub> (L-type) <sup>c</sup>	0 (85.2)	0 (100)	0
Ru(SO <sub>2</sub> )Cl(NO)(PH <sub>3</sub> ) <sub>2</sub> ( $\pi$ -type)	0 (50.3)	-1 (95.2)	0
Mo(CH <sub>2</sub> )(OtBu) <sub>2</sub> (NC <sub>8</sub> H <sub>10</sub> ) (Schrock-type)	-2 (63.0)	0 (33.1)	-2
W(CF <sub>2</sub> )(CO) <sub>5</sub> (Fischer-type)	0 (96.6)	-1 (74.1)	-2/0

<sup>a</sup>The values of R and CI indices are in parentheses. <sup>b</sup>OS of the O atom: 0 (EOS), -1 (LOBA), and -2 (IUPAC). <sup>c</sup>OS of Ru atom: +1 (EOS), +2 (LOBA), and 0 (IUPAC).

summarizes the results obtained with both approaches for all systems considered. The OS is a chemically useful concept that, much like aromaticity, does not have a unique definition. Ultimately, all approaches that aim to assign an integer OS will become ambiguous in regimes where the results approach the boundaries associated with a given assignment. This aspect is reflected in the very useful reliability index (R) of the EOS procedure. Here we have introduced a clarity index to quantify the extent to which a LOBA OS is clear. The CI<sub>a</sub> index approaches 100 away from the ionic/covalent boundary and approaches 0 as the boundary is approached from above or below.

We observed how both EOS and LOBA methods operate synergistically for assigning OS. In the EOS approach, covalent assignments are rare, as there is no EFO occupancy difference range where the assignment is considered shared pair. In

contrast, the LOBA scheme opens a range of population analysis differences (and orbital shape evaluation), where the covalent assignment presents some weight. This is illustrated by the ostensibly simple molecule (CH<sub>3</sub>)<sub>3</sub>NO, for which IUPAC, EOS, and LOBA arrive at different results. Close inspection of the localized orbitals reveals that the LOBA assignment of CH<sub>3</sub> (0), N (+1), and O (-1) relies strongly on covalent character in the bonding, which is not available in EOS.

For the high-valence transition metal oxides culminating with IrO<sub>4</sub><sup>+</sup> and PtO<sub>4</sub><sup>2+</sup> which have IUPAC oxidation states of (+9) and (+10), the latter assignment is neither supported by EOS nor LOBA. LOBA illustrates how delicate these high oxidation states are. With each M–O bond equivalent, LOBA predicts Ir (+9) with low clarity (i.e., O (-2)) and Pt (+6) with higher clarity (i.e., O (-1)) as these systems traverse the ionic/covalent threshold.

Other challenging systems such as a Schrock and a Fisher transition metal carbene complexes show impressive successes for EOS and results that do not match conventional wisdom for LOBA. Relatively low CI<sub>a</sub> values provide a warning that one should carefully inspect the orbitals to assess the LOBA results.

The primary challenge for the LOBA approach is the nonuniqueness of the localization procedure, and the fact that the orbitals in some systems do not localize cleanly. If the final goal is to properly scrutinize the OS of both the ligands and the TM, one should probably incorporate the definition of fragments already when performing the orbital localization, for instance by using fragment populations instead of atomic ones in the localization functional.

Overall, our results cannot be taken as an overall endorsement of any single approach to defining an OS, be it IUPAC, EOS, or LOBA. All these methods will typically agree in straightforward cases (which we have avoided here). In the less straightforward cases, comparing the assignments of all three methods is instructive as a guide to three complementary, and often convergent ways to characterize complex bonding in the simplest possible way. When they differ, it is typically a signature of some interesting complexity or, otherwise, a limitation of one of the approaches.

## COMPUTATIONAL DETAILS

Geometry optimizations were performed by using the  $\omega$ B97X-V density functional<sup>39</sup> coupled with the def2-TZVP basis set (all electron for light atoms and with def2-ECP pseudopotential for heavy atoms).<sup>40</sup> Vibrational frequency calculations, to confirm minima on the potential energy surface, were computed at the same level of theory. Wave functions, orbital localization, and energies were also evaluated at the same level. All calculations were performed with the Q-Chem package.<sup>41</sup>

Localized orbitals bonding analysis (LOBA) calculations were performed with the Q-Chem software, employing the Pipek–Mezey<sup>16</sup> localization procedure, which maximize the locality of Mulliken populations, in conjunction with Löwdin population analysis for each localized orbital, one by one.<sup>19</sup>

Spin-resolved effective fragment orbitals (EFOs) and effective oxidation states (EOS) analysis have been obtained with the APOST-3D program,<sup>42</sup> using the Topological Fuzzy Voronoi Cells (TFVC) 3D-space partitioning method<sup>43</sup> and a 40 × 146 atomic grid for numerical integrations.

## ■ ASSOCIATED CONTENT

## SI Supporting Information

The Supporting Information is available free of charge at <https://pubs.acs.org/doi/10.1021/acs.inorgchem.0c02405>.

Cartesian coordinates of all optimized species (XYZ)

## ■ AUTHOR INFORMATION

## Corresponding Author

**Martin Head-Gordon** – Department of Chemistry, University of California, Berkeley, Berkeley, California 94720, United States; Chemical Sciences Division, Lawrence Berkeley National Laboratory, Berkeley, California 94720, United States; [orcid.org/0000-0002-4309-6669](https://orcid.org/0000-0002-4309-6669); Email: [mhg@cchem.berkeley.edu](mailto:mhg@cchem.berkeley.edu)

## Authors

**Martí Gimferrer** – Institut de Química Computacional i Catàlisi and Departament de Química, Universitat de Girona, 17003 Girona, Catalonia, Spain; [orcid.org/0000-0001-5222-2201](https://orcid.org/0000-0001-5222-2201)

**Jeroen Van der Mynsbrugge** – Department of Chemical and Biomolecular Engineering, University of California, Berkeley, Berkeley, California 94720, United States; [orcid.org/0000-0003-3852-4726](https://orcid.org/0000-0003-3852-4726)

**Alexis T. Bell** – Department of Chemical and Biomolecular Engineering, University of California, Berkeley, Berkeley, California 94720, United States; [orcid.org/0000-0002-5738-4645](https://orcid.org/0000-0002-5738-4645)

**Pedro Salvador** – Institut de Química Computacional i Catàlisi and Departament de Química, Universitat de Girona, 17003 Girona, Catalonia, Spain; [orcid.org/0000-0003-1823-7295](https://orcid.org/0000-0003-1823-7295)

Complete contact information is available at: <https://pubs.acs.org/doi/10.1021/acs.inorgchem.0c02405>

## Notes

The authors declare the following competing financial interest(s): M.H.-G. is a part-owner of Q-Chem Inc., whose software was used for part of this research.

## ■ ACKNOWLEDGMENTS

M.G. thanks the Generalitat de Catalunya and Fons Social Europeu for the predoctoral fellowship (2018 FI\_B 01120). P.S. was supported by the Ministerio de Ciencia, Innovación y Universidades (MCIU), Grant PGC2018-098212-B-C22, and J.V.d.M. was supported by the U.S. Department of Energy's Office of Energy Efficiency and Renewable Energy (EERE) under the Vehicle Technologies Program Award DE-EE0008213. A.T.B. and M.H.G. were supported by the U.S. Department of Energy, Office of Science, Office of Advanced Scientific Computing Research, Scientific Discovery through Advanced Computing (SciDAC) program.

## ■ REFERENCES

- (1) Karen, P.; McArdle, P.; Takats, J. Toward a comprehensive definition of oxidation state (IUPAC Technical Report). *Pure Appl. Chem.* **2014**, *86* (6), 1017–1081.
- (2) Karen, P.; McArdle, P.; Takats, J. Comprehensive definition of oxidation state (IUPAC Recommendations 2016). *Pure Appl. Chem.* **2016**, *88* (8), 831–839.
- (3) Mann, J. B.; Meek, T. L.; Allen, L. C. Configuration energies of the main group elements. *J. Am. Chem. Soc.* **2000**, *122*, 2780–2783.

- (4) Postils, V.; Delgado-Alonso, C.; Luis, J. M.; Salvador, P. An objective alternative to IUPAC's approach to assign oxidation states. *Angew. Chem.* **2018**, *130*, 10685–10689.

- (5) Monsch, G.; Klufers, P.  $[\text{Fe}(\text{H}_2\text{O})_5(\text{NO})]^{2+}$ , a “brown-ring” chromophore. *Angew. Chem., Int. Ed.* **2019**, *58*, 8566–8571.

- (6) Gimferrer, M.; Salvador, P.; Poater, A. Computational monitoring of oxidation states in olefin metathesis. *Organometallics* **2019**, *38*, 4585–4592.

- (7) Ampfeler, T.; Monsch, G.; Popp, J.; Riggenmann, T.; Salvador, P.; Schröder, D.; Klufers, P. Not guilty on every count: the “non-innocent” nitrosyl ligand in the framework of IUPAC's oxidation-state formalism. *Angew. Chem., Int. Ed.* **2020**, *59*, 12381–12386.

- (8) McCleverty, J. A. Chemistry of nitric oxide relevant to biology. *Chem. Rev.* **2004**, *104*, 403–418.

- (9) Resta, R. Charge states in transition. *Nature* **2008**, *453*, 735.

- (10) Raebiger, H.; Lany, S.; Zunger, A. Charge self-regulation upon changing the oxidation state of transition metals in insulators. *Nature* **2008**, *453*, 763–766.

- (11) Walsh, A.; Sokol, A. A.; Buckeridge, J.; Scanlon, D. O.; Catlow, C. R. A. Electron counting in solids: Oxidation states, partial charges, and ionicity. *J. Phys. Chem. Lett.* **2017**, *8*, 2074–2075.

- (12) Thom, A. J. W.; Sundstrom, E. J.; Head-Gordon, M. LOBA: A localized orbital bonding analysis to calculate oxidation states, with application to a model water oxidation catalyst. *Phys. Chem. Chem. Phys.* **2009**, *11*, 11297–11304.

- (13) Sit, P. H.-L.; Zipoli, F.; Chen, J.; Car, R.; Cohen, M. H.; Selloni, A. Oxidation state changes and electron flow in enzymatic catalysis and electrocatalysis through Wannier-function analysis. *Chem. - Eur. J.* **2011**, *17*, 12136–12143.

- (14) Vidossich, P.; Lledos, A. The use of localised orbitals for the bonding and mechanistic analysis of organometallic compounds. *Dalton Trans.* **2014**, *43*, 11145–11151.

- (15) Gimferrer, M.; Comas-Vila, G.; Salvador, P. Can we safely obtain formal oxidation states from centroids of localized orbitals? *Molecules* **2020**, *25*, 234.

- (16) Pipek, J.; Mezey, P. G. A fast intrinsic localization procedure applicable for ab-initio and semiempirical linear combination of atomic orbital wave functions. *J. Chem. Phys.* **1989**, *90*, 4916–4926.

- (17) Edmiston, C.; Ruedenberg, K. Localized atomic and molecular orbitals. *Rev. Mod. Phys.* **1963**, *35*, 457–465.

- (18) Mulliken, R. S. Electronic population analysis on LCAO-MO molecular wave functions. I. *J. Chem. Phys.* **1955**, *23*, 1833–1840.

- (19) Löwdin, P. O. On the nonorthogonality problem connected with the use of atomic wave functions in the theory of molecules and crystals. *J. Chem. Phys.* **1950**, *18*, 365–375.

- (20) Heidar-Zadeh, F.; Ayers, P. W.; Verstraelen, T.; Vinogradov, I.; Vohringer-Martinez, E.; Bultinck, P. Information-theoretic approaches to atoms-in-molecules: Hirshfeld family of partitioning schemes. *J. Phys. Chem. A* **2018**, *122*, 4219–4245.

- (21) Marzari, N.; Vanderbilt, D. Maximally localized generalized Wannier functions for composite energy bands. *Phys. Rev. B: Condens. Matter Mater. Phys.* **1997**, *56*, 12847–12865.

- (22) Ramos-Cordoba, E.; Postils, V.; Salvador, P. Oxidation states from wave function analysis. *J. Chem. Theory Comput.* **2015**, *11*, 1501–1508.

- (23) Mayer, I. Atomic orbitals from molecular wave functions: The effective minimal basis. *J. Phys. Chem.* **1996**, *100*, 6249–6257.

- (24) Ramos-Cordoba, E.; Salvador, P.; Mayer, I. The atomic orbitals of the topological atom. *J. Chem. Phys.* **2013**, *138*, 214107.

- (25) Min, X.; Popov, I. A.; Pan, F.-X.; Li, L.-J.; Matito, E.; Sun, Z.-M.; Wang, L.-S.; Boldyrev, A. I. All-metal antiaromaticity in Sb<sub>4</sub>-type lanthanocene anions. *Angew. Chem., Int. Ed.* **2016**, *55*, 5531–5535.

- (26) Panetier, J. A.; Letko, C. S.; Tilley, D.; Head-Gordon, M. Computational characterization of redox non-innocence in cobalt-bis(diaryldithiolene)-catalyzed proton reduction. *J. Chem. Theory Comput.* **2016**, *12*, 223–230.

- (27) Steen, J. S.; Knizia, G.; Klein, J. E. M. N.  $\sigma$ -Noninnocence: Masked phenyl-cation transfer at formal Ni<sup>IV</sup>. *Angew. Chem., Int. Ed.* **2019**, *58*, 13133–13139.

- (28) Scrocco, M. X-ray photoelectron spectra of Ti<sup>4+</sup> in TiO<sub>2</sub>. Evidence of band structure. *Chem. Phys. Lett.* **1979**, *61*, 453–456.
- (29) Yu, H. S.; Truhlar, D. G. Oxidation state 10 exists. *Angew. Chem., Int. Ed.* **2016**, *55*, 9004–9006.
- (30) Davison, A.; Edelstein, N.; Holm, R. H.; Maki, A. H. The preparation and characterization of four-coordinate complexes related by electron-transfer reactions. *Inorg. Chem.* **1963**, *2*, 1227–1232.
- (31) Lim, B. S.; Fomitchov, D. V.; Holm, R. H. Nickel dithiolenes revisited: structures and electron distribution from density functional theory for the three-member electron-transfer series [Ni(S<sub>2</sub>C<sub>2</sub>Me<sub>2</sub>)<sub>2</sub>]<sup>0,1,2-</sup>. *Inorg. Chem.* **2001**, *40*, 4257–4262.
- (32) Karen, P. Oxidation state, a long-standing issue! *Angew. Chem., Int. Ed.* **2015**, *54*, 4716–4726.
- (33) Snyder, J. P. Elusiveness of Cu(III) complexation; preference for trifluoromethyl oxidation in the formation of [Cu<sup>I</sup>(CF<sub>3</sub>)<sub>4</sub>]<sup>-</sup> salts. *Angew. Chem., Int. Ed. Engl.* **1995**, *34*, 80–81.
- (34) Kaupp, M.; von Schnering, H. G. Formal oxidation state versus partial charge - A comment. *Angew. Chem., Int. Ed. Engl.* **1995**, *34*, 986.
- (35) Aullón, G.; Alvarez, S. Oxidation states, atomic charges and orbital populations in transition metal complexes. *Theor. Chem. Acc.* **2009**, *123*, 67–73.
- (36) Walroth, R. C.; Lukens, J. T.; MacMillan, S. N.; Finkelstein, K. D.; Lancaster, K. M. Spectroscopic evidence for a 3d<sup>10</sup> ground state electronic configuration and ligand field inversion in [Cu(CF<sub>3</sub>)<sub>4</sub>]<sup>1-</sup>. *J. Am. Chem. Soc.* **2016**, *138*, 1922–1931.
- (37) DiMucci, I. M.; Lukens, J. T.; Chatterjee, S.; Carsch, K. M.; Titus, C. J.; Lee, S. J.; Nordlund, D.; Betley, T. A.; MacMillan, S. M.; Lancaster, K. M. The myth of d<sup>8</sup> copper(III). *J. Am. Chem. Soc.* **2019**, *141*, 18508–18520.
- (38) Hoffmann, R.; Alvarez, S.; Mealli, C.; Falceto, A.; Cahill, T. J., III; Zeng, T.; Manca, G. From widely accepted concepts in coordination chemistry to inverted ligand fields. *Chem. Rev.* **2016**, *116*, 8173–8192.
- (39) Mardirossian, N.; Head-Gordon, M. ωB97X-V: A 10-parameter, range-separated hybrid, generalized gradient approximation density functional with nonlocal correlation, designed by a survival-of-the-fittest strategy. *Phys. Chem. Chem. Phys.* **2014**, *16*, 9904–9924.
- (40) Weigend, W.; Ahlrichs, R. Balanced basis sets of split valence, triple zeta valence and quadruple zeta valence quality for H to Rn: Design and assessment of accuracy. *Phys. Chem. Chem. Phys.* **2005**, *7*, 3297.
- (41) Shao, Y.; Gan, Z.; Epifanovsky, E.; Gilbert, A. T. B.; Wormit, M.; Kussmann, J.; Lange, A. W.; Behn, A.; Deng, J.; Feng, X.; Ghosh, D.; Goldey, M.; Horn, P. R.; Jacobson, L. D.; Kaliman, I.; Khaliullin, R. Z.; Kus, T.; Landau, A.; Liu, J.; Proynov, E. I.; Rhee, Y. M.; Richard, R. M.; Rohrdanz, M. A.; Steele, R. P.; Sundstrom, E. J.; Woodcock, H. L.; Zimmerman, P. M.; Zuev, D.; Albrecht, B.; Alguire, E.; Austin, B.; Beran, G. J. O.; Bernard, Y. A.; Berquist, E.; Brandhorst, K.; Bravaya, K. B.; Brown, S. T.; Casanova, D.; Chang, C.-M.; Chen, Y.; Chien, S. H.; Closser, K. D.; Crittenden, D. L.; Diedenhofen, M.; DiStasio, R. A.; Do, H.; Dutoi, A. D.; Edgar, R. G.; Fatehi, S.; Fusti-Molnar, L.; Ghysels, A.; Golubeva-Zadorozhnaya, A.; Gomes, J.; Hanson-Heine, M. W. D.; Harbach, P. H. P.; Hauser, A. W.; Hohenstein, E. G.; Holden, Z. C.; Jagau, T.-C.; Ji, H.; Kaduk, B.; Khistyayev, K.; Kim, J.; Kim, J.; King, R. A.; Klunzinger, P.; Kosenkov, D.; Kowalczyk, T.; Krauter, C. M.; Lao, K. U.; Laurent, A. D.; Lawler, K. V.; Levchenko, S. V.; Lin, C. Y.; Liu, F.; Livshits, E.; Lochan, R. C.; Luenser, A.; Manohar, P.; Manzer, S. F.; Mao, S.-P.; Mardirossian, N.; Marenich, A. V.; Maurer, S. A.; Mayhall, N. J.; Neuscammann, E.; Oana, C. M.; Olivares-Amaya, R.; O'Neill, D. P.; Parkhill, J. A.; Perrine, T. M.; Peverati, R.; Prociuk, A.; Rehn, D. R.; Rosta, E.; Russ, N. J.; Sharada, S. M.; Sharma, S.; Small, D. W.; Sodt, A.; Stein, T.; Stück, D.; Su, Y.-C.; Thom, A. J. W.; Tsuchimochi, T.; Vanovschi, V.; Vogt, L.; Vydrov, O.; Wang, T.; Watson, M. A.; Wenzel, J.; White, A.; Williams, C. F.; Yang, J.; Yeganeh, S.; Yost, S. R.; You, Z.-Q.; Zhang, I. Y.; Zhang, X.; Zhao, Y.; Brooks, B. R.; Chan, G. K. L.; Chipman, D. M.; Cramer, C. J.; Goddard, W. A.; Gordon, M. S.; Hehre, W. J.; Klamt, A.; Schaefer, H. F.; Schmidt, M. W.; Sherrill, C. D.; Truhlar, D. G.; Warshel, A.; Xu, X.; Aspuru-Guzik, A.; Baer, R.; Bell, A. T.; Besley, N. A.; Chai, J.-D.; Dreuw, A.; Dunietz, B. D.; Furlani, T. R.; Gwaltney, S. R.; Hsu, C.-P.; Jung, Y.; Kong, J.; Lambrecht, D. S.; Liang, W.; Ochsenfeld, C.; Rassolov, V. A.; Slipchenko, L. V.; Subotnik, J. E.; Van Voorhis, T.; Herbert, J. M.; Krylov, A. I.; Gill, P. M. W.; Head-Gordon, M. Advances in molecular quantum chemistry contained in the Q-Chem 4 program package. *Mol. Phys.* **2015**, *113*, 184.
- (42) Salvador, P.; Ramos-Cordoba, E.; Gimferrer, M. *APOST-3D Program*; Universitat de Girona: Girona, Spain, 2019.
- (43) Salvador, P.; Ramos-Cordoba, E. An approximation to Bader's topological atom. *J. Chem. Phys.* **2013**, *139*, 071103.